Available online at www.sciencedirect.com
SCIENCE DIRECT®
International Journal of Heat and Fluid Flow 25 (2004) 721–728
International Journal of HEAT AND FLUID FLOW
www.elsevier.com/locate/ijhff

Influence of particle rotation on the interaction between particle clusters and particle-induced turbulence

Takeo Kajishima

Department of Mechanical Engineering, Osaka University, Suita, Osaka 565-0871, Japan

Received 9 January 2004; accepted 5 May 2004
Available online 4 July 2004

Abstract

To investigate the collective behavior of solid particles in the particle-induced turbulence, a direct numerical simulation of homogeneous flow including a lot of settling particles was conducted. The flow around each particle was fully resolved by the finite-difference method. A particle was assumed to be rigid and spherical. The number of solid particles was up to 2048 and the number of grid for fluid flow was 268 millions. Particles moving with Reynolds number 300 formed clusters (high-concentration regions) due to wake-attractions. Influences of the loading ratio and particle rotation were particularly investigated. The rotation drastically affected numerical results. Irrotational particles were absorbed into clusters but rotational ones escaped. Such difference was caused by reverse direction of lift in the shear flows. Moreover, it was found that the particle-induced turbulence became severalfold of the total of disturbance by vortex shedding from each particle when particles formed clusters.

Keywords: Multiphase flow; Turbulent flow; Particle-laden turbulence; Wake; Direct numerical simulation; Particle rotation; Cluster

1. Introduction

Solid particles significantly affect the transfer of momentum, heat and mass in turbulent flows. Extensive researches have therefore been conducted for the turbulence modulation by particles (Gore and Crowe, 1989; Elghobashi, 1994). The direct numerical simulation (DNS) is hopeful for such a purpose because the simultaneous measurement for particle motion and fluid force on the particle is difficult in experiment. DNS principally deal with all physics involved in a computational domain. Thus, in order to investigate the turbulence modulation by particles, flow around each particle should be resolved, avoiding the use of any empirical point-source models for particle motion.

The interaction in larger scale is more dominant for turbulence modulation. The largest scale is not close to the particle size but it is related to the particle distribution. So the non-uniformity in particle distribution is particularly considered, in the multiple-scale interactions between particles and turbulence. The objective of this study is to clarify the dominant factors for the collective behaviors of particles. Especially, the influences of loading ratio and rotation of particles are considered.

Hereafter particles are assumed to be rigid spheres of uniform diameter. The sphere is the simplest three-dimensional shape, but the flow around it has quite a wide variation, even for the fixed particle in a uniform stream, as known experimentally (Achenbach, 1974; Sakamoto and Haniu, 1990) and numerically (Shirayama, 1992; Johnson and Patel, 1999). They suggested the pattern of wake as follows, but one must note that there remains some diversity in critical Reynolds numbers. A steady and axisymmetric vortex ring attaches at the sphere for Reynolds number, based on the sphere diameter and relative velocity, less than approximately 210. A vortex ring becomes non-axisymmetric, but steady and plane-symmetric, for Re between 210 and 270. For the Reynolds number greater than approximately 270, the unsteady vortex shedding takes place. The orientation and period of vortex shedding seems nearly constant for $Re \simeq 300$ but they become more random for higher Reynolds number. The present study deals with the Reynolds number at around 300. The

E-mail address: kajisima@mech.eng.osaka-u.ac.jp (T. Kajishima).

0142-727X/$ - see front matter © 2004 Elsevier Inc. All rights reserved.
doi:10.1016/j.ijheatfluidflow.2004.05.007

above-mentioned patterns have been successfully reproduced by our method (Takiguchi et al., 1999; Kajishima et al., 2001), which will be outlined below.

This paper reports DNS results for interactive phenomenon between particles settling by gravity and flow induced by them in a homogeneous domain. First, the numerical method for full-scale computation from flow around particle to particle-induced turbulence is summarized. Then results are discussed from a viewpoint of particle distribution. Particular attention is focused on the factors of loading ratio and rotation of particles. Especially the latter was not accounted for in our previous work (Kajishima and Takiguchi, 2002) and it might have been often ignored or inaccurately treated in previous simulations.

2. DNS method

2.1. Numerical scheme

A DNS method has been successfully developed for the full scale simulation of flow including thousands of particles moving with the Reynolds number range of vortex shedding (Takiguchi et al., 1999; Kajishima et al., 2001). In this method, flow around each particle is resolved and then the force on particle is evaluated based on the surface integral of fluid stress.

The Cartesian coordinate system is selected for our DNS. The computational mesh, cubic in this study, does not fit the surface of spherical particles. To account for the immersed boundary, we use the volume fraction of the particle in a computational cell that includes solid–fluid interface. The volume-weighted average of velocity $\boldsymbol{u} = \alpha \boldsymbol{u}_\mathrm{p} + (1-\alpha)\boldsymbol{u}_\mathrm{f}$ is defined for two-way coupling. α represents the volume fraction of the solid in the computational cell, $\boldsymbol{u}_\mathrm{f}$ the fluid velocity, $\boldsymbol{u}_\mathrm{p}(= \boldsymbol{v}_\mathrm{p} + \boldsymbol{\omega}_\mathrm{p} \times \boldsymbol{r}$: the second term was mistyped but not used in Kajishima and Takiguchi, 2002) the velocity inside the solid body moving with translational velocity $\boldsymbol{v}_\mathrm{p}$ and angular velocity $\boldsymbol{\omega}_\mathrm{p}$. $\boldsymbol{r}$ denotes the relative position from the center of rotation. Considering the Navier–Stokes equation for $\boldsymbol{u}_\mathrm{f}$, we give a governing equation for $\boldsymbol{u}$ by

$$\frac{\partial \boldsymbol{u}}{\partial t} = -\nabla \frac{p}{\rho_\mathrm{f}} - \boldsymbol{u}\cdot\nabla\boldsymbol{u} + \nu_\mathrm{f}\nabla^2\boldsymbol{u} + \boldsymbol{f}_\mathrm{p}, \tag{1}$$

where ρ_f is the fluid density and ν_f the kinematic viscosity. They are assumed to be constant. The additional term is $\boldsymbol{f}_\mathrm{p} = \alpha(\boldsymbol{u}_\mathrm{p} - \hat{\boldsymbol{u}}_\mathrm{f})/\Delta t$, where $\hat{\boldsymbol{u}}_\mathrm{f}$ is a predicted velocity through the Navier–Stokes equation for $\boldsymbol{u}_\mathrm{f}$ and Δt the time-increment. The value of $\boldsymbol{f}_\mathrm{p}$ is meaningful in a cell of $\alpha > 0$ so as to represent the momentum exchange between the phases (Kajishima et al., 2001).

The integral of the fluid stress on the particle surface can be replaced by the volume integral of $\boldsymbol{f}_\mathrm{p}$ (Kajishima et al., 2001). Thus the equations of translational and rotational motion of a particle become

$$\frac{\mathrm{d}(m_\mathrm{p}\boldsymbol{v}_\mathrm{p})}{\mathrm{d}t} = \int_{V_\mathrm{p}} \boldsymbol{f}_\mathrm{p}\,\mathrm{d}V + \boldsymbol{g}_\mathrm{p}, \tag{2}$$

$$\frac{\mathrm{d}(\boldsymbol{I}_\mathrm{p}\cdot\boldsymbol{\omega}_\mathrm{p})}{\mathrm{d}t} = \int_{V_\mathrm{p}} \boldsymbol{r}\times\boldsymbol{f}_\mathrm{p}\,\mathrm{d}V + \boldsymbol{h}_\mathrm{p}, \tag{3}$$

where m_p denotes the mass of the particle and $\boldsymbol{I}_\mathrm{p}$ the inertia tensor. The domain V_p can be slightly larger than the particle and it must include all interfacial cells around it. The last terms, $\boldsymbol{g}_\mathrm{p}$ and $\boldsymbol{h}_\mathrm{p}$, are external force and moment, respectively $\boldsymbol{g}_\mathrm{p} = -[(\rho_\mathrm{p}-\rho_\mathrm{f})/\rho_\mathrm{p}]m_\mathrm{p}g\boldsymbol{e}_z$ and $\boldsymbol{h}_\mathrm{p} = 0$ in this computation.

We apply the above method to homogeneous turbulence including spherical particles. Grid points for the simulation of fluid turbulence are distributed uniformly in a periodic computational domain. The spatial derivative is approximated by a central finite-difference method of the fourth-order accuracy. The second-order schemes are applied for time marching, namely the Adams–Bashforth method for the equations of motion for fluid and solid particle and the Crank–Nicholson method for the particle movement. The SMAC method is used for velocity–pressure coupling. More details on the two-way coupling method were given in our previous paper (Kajishima and Takiguchi, 2002).

2.2. Computational setup

The non-dimensional diameter of a particle is $D_\mathrm{p} = 1$. Assuming the settling velocity of a particle in a stationary field to be $U_0 = 1$, the kinematic viscosity of fluid is given as $\nu_\mathrm{f} = D_\mathrm{p}U_0/Re_\mathrm{ps}(= 1/Re_\mathrm{ps})$ by a desired Reynolds number Re_ps. Then the gravitational force is given so as to be balanced with the drag, which is estimated by the standard Re_ps–C_D correlation for a fixed sphere in a uniform flow (Clift et al., 1978). In this calculation, the Reynolds number is $Re_\mathrm{ps} = 300$ and the density ratio is $\rho_\mathrm{p}/\rho_\mathrm{f} = 8.8$. The setup is corresponding to a copper particle having diameter of 0.85 mm in water.

The periodic boundary condition is applied in all directions assuming the uniformity of the flow field. The computational cell is cubic. The number of them is 512 in the horizontal (x, y) directions and 1024 in the vertical (z) direction. The ratio of particle diameter to grid spacing is $D_\mathrm{p}/\Delta = 10$, which allowed sufficient accuracy for vortex shedding at the particle Reynolds number range of interest (Takiguchi et al., 1999; Kajishima et al., 2001). The ratio of the grid spacing to Kolmogorov length scale of particle-induced turbulence is $\Delta/\eta_\mathrm{K} = 2$–$4$. This condition is fairly reasonable to resolve a dissipation scale of turbulence.

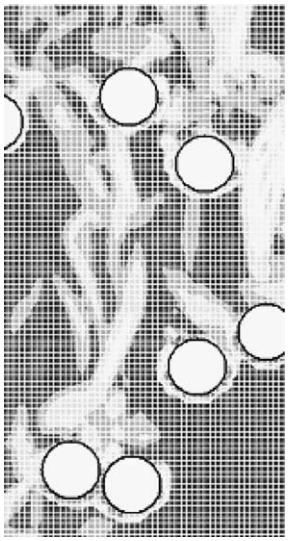

Fig. 1. A part of instantaneous flow field caused by shed vortices from settling spheres: projection of $\nabla^2 p$ in a part of vertical plane and computational grid.

Four cases for the number of solid particles are calculated: $N_\mathrm{p} = 256$, 512, 1024 and 2048. The volume-loading ratio are correspondingly $\Phi = 0.0005$, 0.001, 0.002 and 0.004, respectively. In such a dilute mixture, inter-particle collisions could occur, but are unlikely to dominate the particle distribution and the flow field. Thus, we assume elastic collisions for simplicity in this study.

Initially, uniformly distributed particles and fluids are at rest. Hence, particles fall down by gravity. To keep the mass flow rate of the mixture at zero, we add a constant vertical gradient of pressure in the equation of fluid motion.

Fig. 1 shows an example of instantaneous flow field obtained for $N_\mathrm{p} = 1024$. The resolution can be evaluated from this figure. Local low pressure regions are indicated by the contour of $\nabla^2 p$. It is often used for the visualization of vortical motion. Due to the immersed boundary method on the Cartesian coordinate system, the vicinity of particle is somewhat noisy. However, hairpin vortices shed from particles are smoothly captured in this calculation.

3. Results and discussion

The influence of Reynolds number on the collective behavior of solid particles has already reported (Kajishima and Takiguchi, 2002). Thus particular attentions are focused on the rotation and loading ratio of particles in this section. A particle released in fluid is of course 'rotational'. On the other hand, the computation in which the particle rotation is ignored is hereafter denoted as 'irrotational'. An irrotational particle is hypothetical situation for the investigation of a particular factor, which is possible only in the computational simulation.

3.1. Time evolution of flow field

Fig. 2 shows time evolutions of averaged Reynolds number Re_p of settling particles. Re_p is based on the average slip velocity, which is different from Re_ps because of the collective behavior of particles. For most cases, average Reynolds number of particles Re_p becomes larger than $Re_\mathrm{ps}(= 300)$ and the temporal fluctuation is significant. The increase in settling speed is approximately 20% for irrotational particles and it does not depend on the particle loading ratio. The increase for rotational particles is slightly smaller than that for irrotational ones. Furthermore, the motion of rotational particles is significantly affected by the loading ratio.

Fig. 3 shows time evolutions of mean distance to the nearest particles, L_p. After the developed stage is reached in $tU_0/D_\mathrm{p} \gtrsim 2000$, the inter-particle distance decreases when Re_p in Fig. 2 increases. This negative correlation between L_p and Re_p suggests the falling

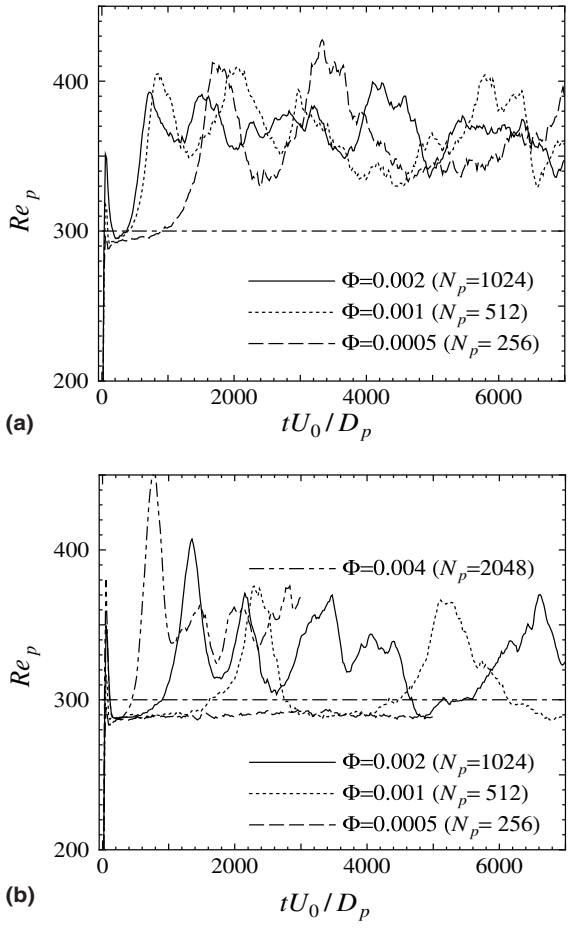

Fig. 2. Average Reynolds number of particles, based on slip velocity and diameter. (a) Irrotational particles; (b) rotational particles.

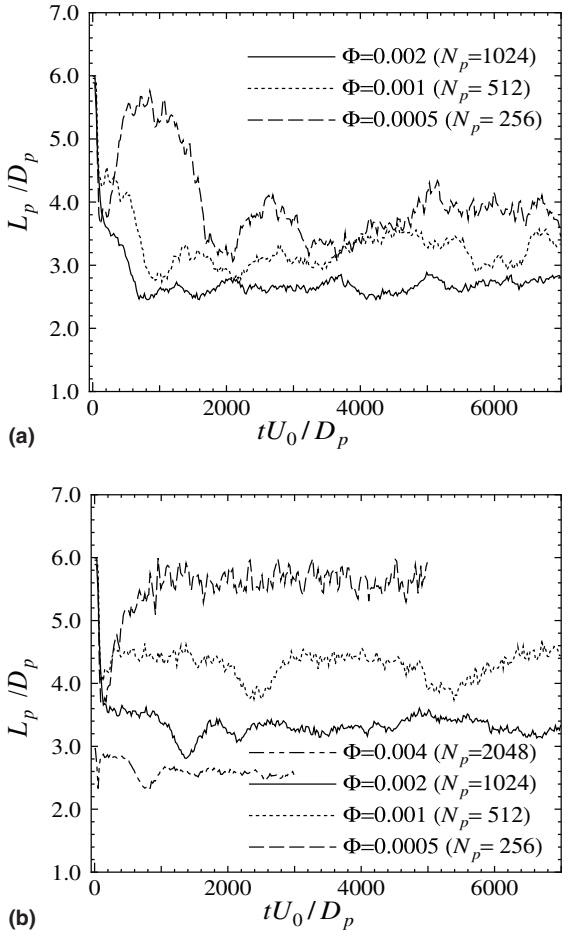

Fig. 3. Average distance to the nearest particle. (a) Irrotational particles; (b) rotational particles.

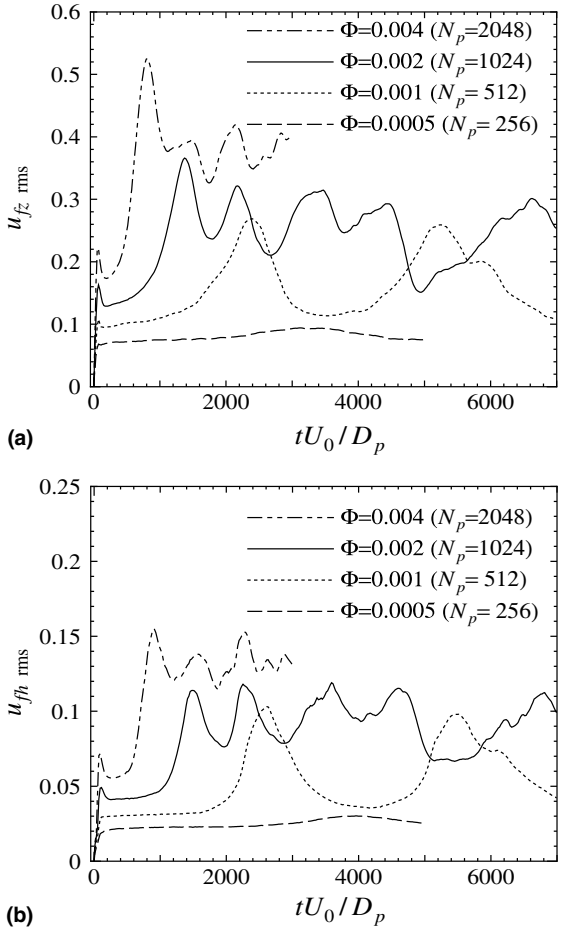

Fig. 4. Intensity of fluid velocity fluctuation due to rotational particles. (a) Vertical component; (b) horizontal component.

velocity becomes larger when particles form high-density regions. In this paper, such a region of particles is denoted as 'cluster'. The drag on a particle trapped into the wake of the other becomes smaller and it reaches to the other. Such a 'wake-attraction' is the mechanism of clustering in our case (Kajishima and Takiguchi, 2002). Since many particles have less drag in the cluster, the average Reynolds number increases. Clusters of irrotational particles seem to be maintained continuously. For rotational ones, on the other hand, the collective behavior is much affected by the loading ratio. The dilute addition cannot form clusters. In this case, Re_s of separately falling particles at $\Phi = 0.0005$ is smaller than Re_{ps}. This may be due to the drag increase by turbulence effect. According to the increase in loading ratio of rotational particles, clusters develop and then break up periodically at $\Phi = 0.001$. The period becomes shorter and more irregular for higher loading ratio.

Fig. 4 shows time evolutions of intensities of fluid turbulence (root-mean-square values) caused by rotational particles. There exists close correlation between fluid turbulence and particle distribution in case of $\Phi \geqslant 0.001$. By comparing Figs. 2(b) and 4(a), velocity fluctuation in the vertical (z) direction $v_{fz\,\mathrm{rms}}$ increases with slight delay of increase in particle Reynolds number due to clustering. Then the horizontal ($h = x, y$) component $v_{fh\,\mathrm{rms}}$ follows with additional delay as shown in Fig. 4(b). The averaged ratio of $v_{fz\,\mathrm{rms}}/v_{fh\,\mathrm{rms}}$ is, roughly speaking, 3 and this value is similar to the ratio between mainstream and lateral components in turbulent flows along a plane wall. This horizontal fluctuation can be a cause for the break-up of clusters (Kajishima and Takiguchi, 2002).

Figs. 2 and 3 shows a clear difference between actual particles and rotation-ignored particles. Irrotational particles keep cluster structure with weak fluctuations. On the other hand, rotational particles cause quasi-periodic formation and break-up of clusters and such a collective behavior is affected by the loading ratio.

To consider the reason of such a difference in collective behavior, Fig. 5 shows the horizontal behavior of particles: namely, time evolution of the intensity of translational and angular velocities. The correlation between Figs. 2(b) and 5(b), particularly for $\Phi = 0.002$

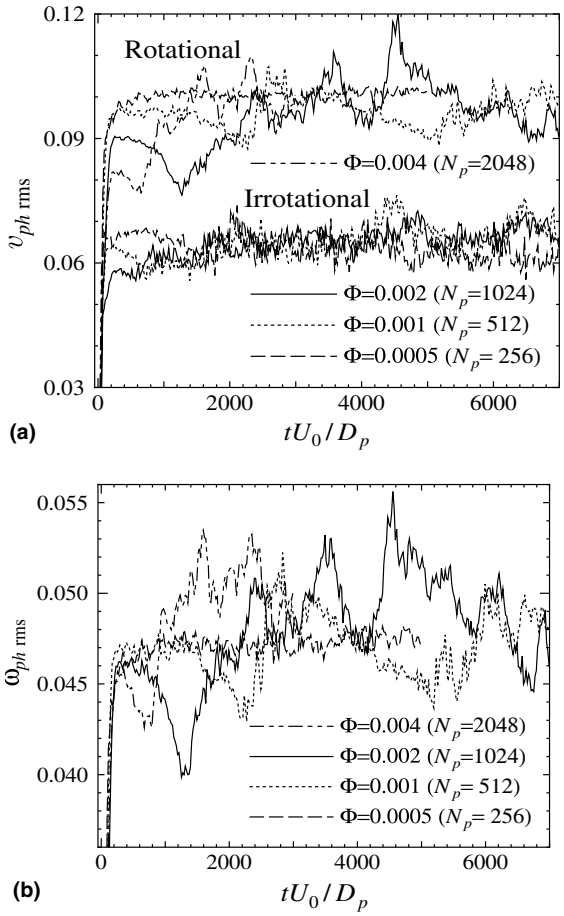

Fig. 5. Horizontal components of translational and angular velocity fluctuations of particles. (a) Translational velocity; (b) angular velocity.

loading and in non-dimensional time from 1000 to 5000, indicate that the rotation $\omega_{ph\,\mathrm{rms}}$ increases gradually in the period of clustering. The angular momentum is generated in high-shear region around clusters, which are falling with high velocity. Thus particles receive continual lift force due to their rotation and tend to slide to horizontal directions as shown in Fig. 5(a). The lift by the rotation obtained in high-shear region acts into the outward direction from clusters as shown later. As a result, clusters are reproduced periodically but cannot be stable in comparison with ones formed by irrotational particles.

Fig. 6 shows the time evolution of energy dissipation rate of fluid turbulence, ε_f. The time-average of ε_f is identical with that of the energy production rate by particles since there is no additional source of turbulence. In the lowest loading case without collective behavior, ε_f is thought to be the total of energy caused by the vortex shedding from each particle. The turbulence intensity does not increase proportionally with the particle loading ratio but becomes several times larger than linear expectation, when particles form clusters.

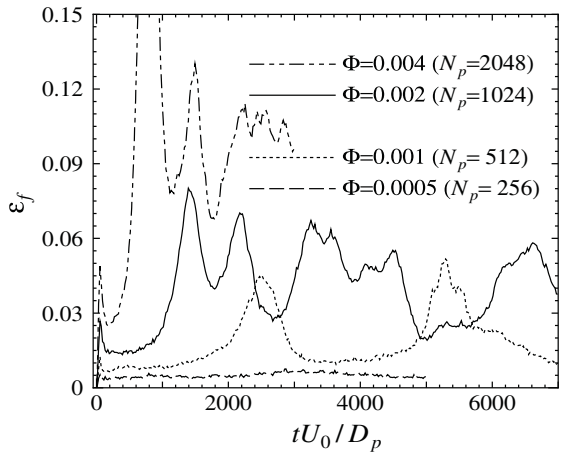

Fig. 6. Energy dissipation rate of fluid turbulence caused by rotational particles.

3.2. Instantaneous distribution of particles

Fig. 7 shows the instantaneous distributions of particles for $\Phi = 0.002$ at the developed stage to compare the effect of particle rotation. Fig. 8 is a projection of irrotational particles shown in Fig. 7(a) to a horizontal plane. Fig. 9 shows horizontal projections for rotational particles at some typical instants. Angular velocity vectors are also included in the figure.

Vertically elongated clusters are observed in Fig. 7(a) and the horizontal scale of them is clear in Fig. 6. Particles trapped in these high-concentration regions fall faster than average. By the movie, one can observe irrotational particles, even if they once drop out from a cluster, return to it or go into another cluster. Clusters behave somewhat dynamically but the structure is maintained.

When the particle rotation is accounted for, firstly developed clusters shown in Fig. 9(a) have similar size and strength with those by irrotational ones shown in Fig. 8. But the break-up is more complete as shown in Fig. 9(b). At the next step, regenerated clusters shown in Fig. 9(c) become larger but the local concentration of particles is lower. During the repetition of this process, the particle rotation grows as shown in Fig. 5(b). Consequently, the high-concentration clusters such as initial ones are never reproduced. By the movie, one can confirm the sliding motion of particle in the horizontal plane is in the direction 90° anticlockwise from its angular velocity vector. Namely, it is due to the Magnus lift force. In the clustering stage, Fig. 9(a) and (c) for example, the angular velocity of particles in the core of high concentration is smaller than that of separated ones.

The difference between rotational and irrotational particles is due to the difference in the direction of lift as schematically shown in Fig. 10. Clusters cause faster

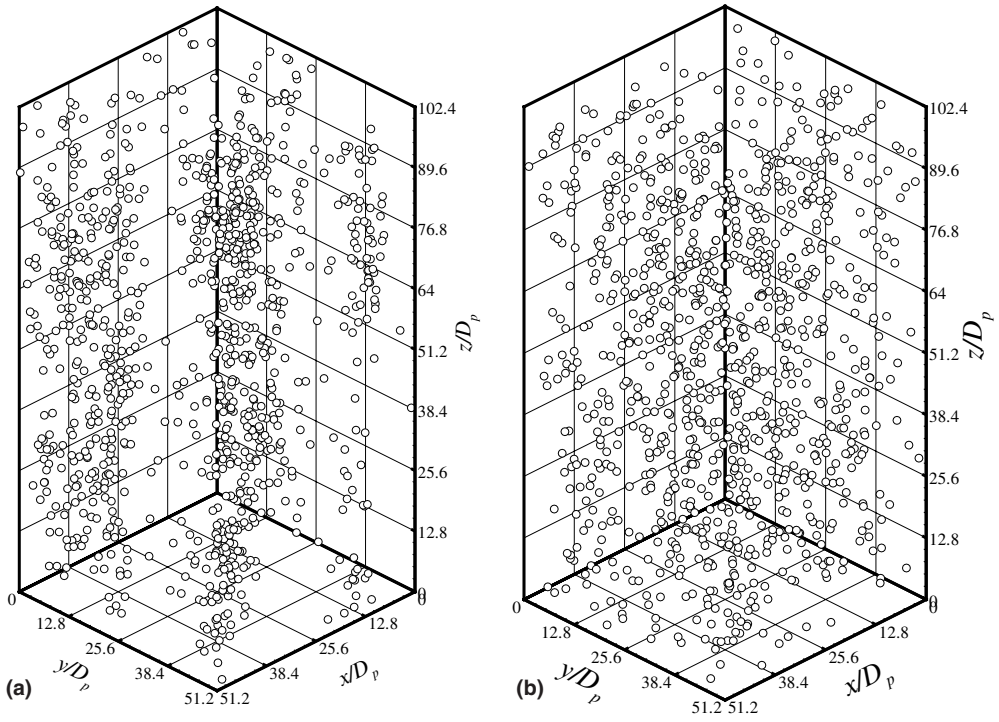

Fig. 7. Instantaneous distribution of particles ($Re_{ps} = 300$, $N_p = 1024$). (a) Irrotational ($t = 3000D_p/U$); (b) rotational ($t = 5000D_p/U$).

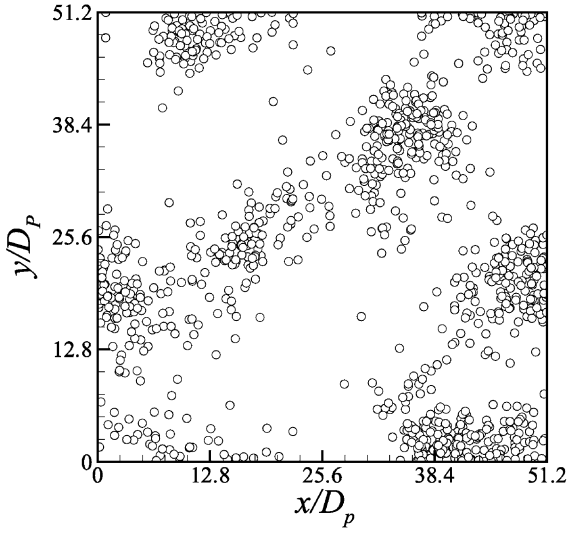

Fig. 8. Horizontal projection of Fig. 7(a).

downward current of fluid and make high-shear layer around them. In this region, particles without rotation receive the lift force to the direction of cluster center, resulting in the absorption. This is corresponding to the finding by Kurose and Komori (1999), in which they reported the lift is in the direction to less relative velocity side for Reynolds number greater than 60. It is opposite to the Saffman lift force model (Saffman, 1965). When particles receive angular momentum in the shear region, the Magnus lift force is in the direction outward from cluster center. In addition, the rotation tends to sustain the sliding motion because the orientation of unsteady vortex shedding tends to be fixed. Then, rotational particles have continuous horizontal motion, which is originally in the direction dropping out from clusters. As a consequence, they travel randomly and unlikely form high-concentration clusters.

4. Conclusion

DNS was applied to elucidate interactions involved in particle-laden turbulent flows. Particular attention was focused on the distribution of particle concentration in this study. This is because temporal and spatial scales related to particle clusters are thought to be the largest scale for energy input to fluid turbulence. From such a viewpoint, efficient and accurate scheme was successfully developed to track thousands of particles. In this calculation, flow around each particle was directly resolved.

In our previous paper (Kajishima and Takiguchi, 2002), it was reported that particle clusters develop when particle Reynolds number based on its diameter and slip velocity is in the range of vortex shedding. In the present study, the influences of particle rotation and loading ratio were discussed for Reynolds number 300. Particles in cluster fell faster than average because of the smaller fluid drag in the wake of other particles. It is due to the high density in mixture, in other words. Then clusters made high-shear region around them resulting in the turbulence

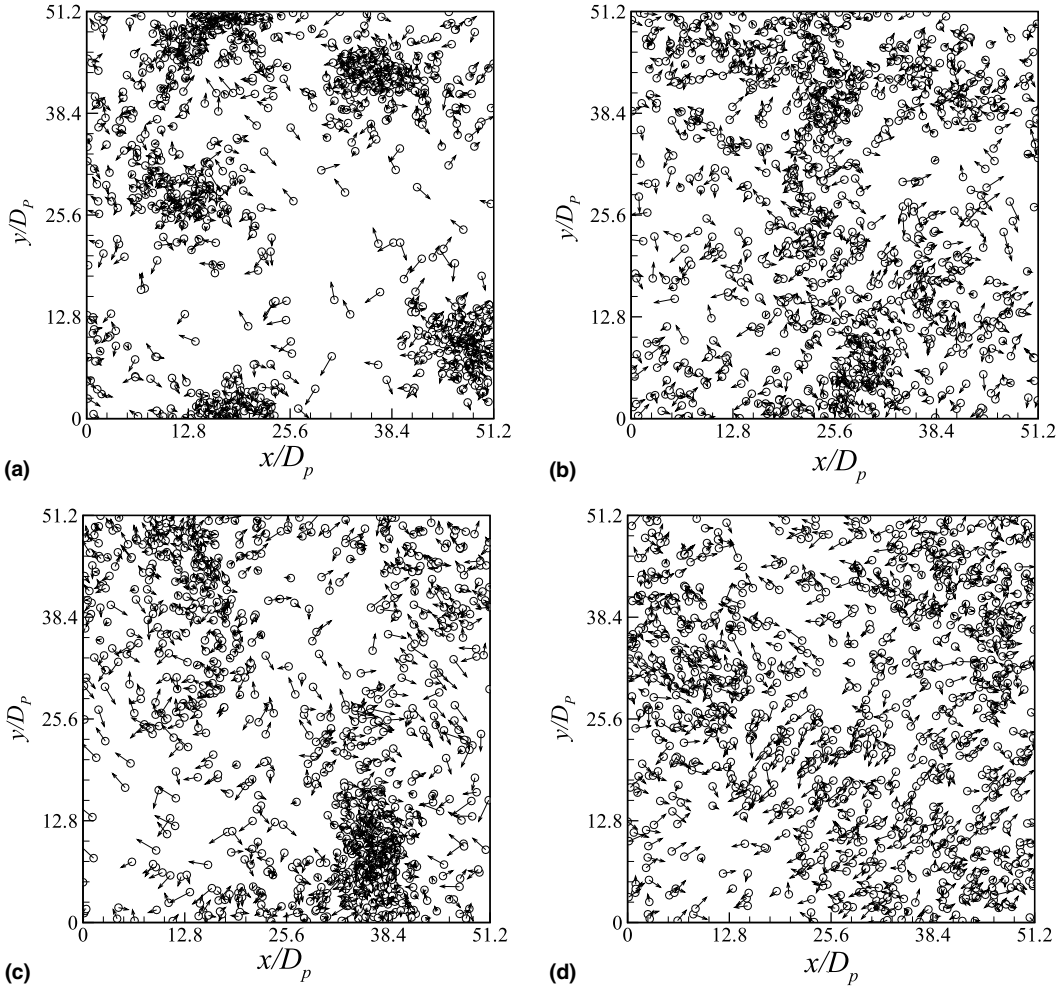

Fig. 9. Horizontal projection of instantaneous distribution and angular velocity of rotational particles ($N_p = 1024$). (a) $t = 1340D_p/U$; (b) $t = 1700D_p/U$; (c) $t = 2200D_p/U$; (d) $t = 5000D_p/U$.

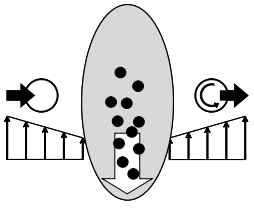

Fig. 10. Lift force on irrotational and rotational particles near a cluster.

production. The effect of particle rotation manifested itself after such a process. Irrotational particles maintained cluster structure while rotational ones moved randomly in the horizontal direction. Moreover, the collective behavior of rotational particles was affected by the loading ratio. The major reason of difference was the direction of lateral component of fluid force, that is lift force. A dominant factor of actual (rotational) particles was Magnus lift force, which was given by the fluid shear and preserved due to the inertia of rotation.

The collective behavior of particles with vortex shedding affected significantly the mean slip velocity, distribution of particle concentration and intensity of particle-induced turbulence. Namely, the cluster structure caused 20% increase in mean slip velocity in this case. Furthermore, fluid turbulence became several times larger than the total contribution of vortices shed from each particle. These results suggest that further improvements of practical models for particle motion and fluid turbulence are necessary.

Acknowledgements

The author tenders his acknowledgment to Dr. Satoshi Takiguchi (Mitsubishi Heavy Industries, Ltd.) who made important contribution to developing the numerical scheme. This work was partially supported by a Grant-in-Aid Scientific Research on Priority Areas (B) No. 12125202 from the Ministry of Education, Culture, Sports, Science and Technology of Japan.

References

Achenbach, E., 1974. Vortex shedding from spheres. J. Fluid Mech. 62 (2), 209–221.

Clift, R., Grace, J.R., Weber, M.E., 1978. Bubbles, Drops and Particles. Academic Press, New York.

Elghobashi, S., 1994. On predicting particle-laden turbulent flows. Appl. Sci. Res. 52, 309–329.

Gore, R.A., Crowe, C.T., 1989. Effect of particle size on modulating turbulence intensity. Int. J. Multiphase Flow 15 (2), 279–285.

Johnson, T.A., Patel, V.C., 1999. Flow past a sphere up to Reynolds number 300. J. Fluid Mech. 378, 19–70.

Kajishima, T., Takiguchi, S., Hamasaki, H., Miyake, Y., 2001. Turbulence structure of particle-laden flow in a vertical plane channel due to vortex shedding. JSME Int. J. Ser. B 44 (4), 526–535.

Kajishima, T., Takiguchi, S., 2002. Interaction between particle clusters and particle-induced turbulence. Int. J. Heat Fluid Flow 23, 639–646.

Kurose, R., Komori, S., 1999. Drag and lift forces on a rotating sphere in a linear shear flow. J. Fluid Mech. 384, 183–206.

Saffman, P.G., 1965. The lift force on a small sphere in a slow shear flow. J. Fluid Mech. 22, 385–400.

Sakamoto, H., Haniu, H., 1990. A study on vortex shedding from spheres in a uniform flow. J. Fluids Eng. 112, 386–392.

Shirayama, S., 1992. Flow past a sphere: topological transitions of the vorticity field. AIAA J. 30 (2), 349–358.

Takiguchi, S., Kajishima, T., Miyake, Y., 1999. Numerical scheme to resolve the interaction between solid-particles and fluid-turbulence. JSME Int. J. Ser. B 42 (3), 411–418.